Research Article | Vol. 11, No. 5 / 1 May 2021 / Optical Materials Express 1489
Optical Materials EXPRESS

Diode-pumped master oscillator power amplifier system based on cryogenically cooled Tm:Y_2O_3 transparent ceramics

FANGXIN YUE,[1,2,3] VENKATESAN JAMBUNATHAN,[1,*] SAMUEL PAUL DAVID,[1] XAVIER MATEOS,[2] JAN ŠULC,[3] MARTIN SMRŽ,[1] AND TOMÁŠ MOCEK[1]

[1]*HiLASE Center, Institute of Physics of the Czech Academy of Sciences, Za Radnicí 828, 25241 Dolní Břežany, Czech Republic*
[2]*Universitat Rovira i Virgili, Física i Cristal·lografia de Materials i Nanomaterials (FiCMA-FiCNA), Marcel·lí Domingo 1, 43007 Tarragona, Spain*
[3]*Faculty of Nuclear Sciences and Phys. Eng., Czech Technical University in Prague, Brehova 7, 11519 Prague, Czech Republic*
[*]*jambunath@fzu.cz*

Abstract: We demonstrated a master oscillator power amplifier system using cryogenically cooled Tm:Y_2O_3 transparent ceramics. The electro-optically switched master oscillator acted as a seed source and could be tuned from 1 to 100 Hz. A maximum pulse energy of 1.35 mJ with a pulse duration of 30 ns amounting to a peak power of 45 kW was obtained at 10 Hz. The power amplification via double-pass geometry achieved maximum single pulse energy of 2.94 mJ at 10 Hz with a pulse duration of 32 ns. The results showed the pulsed lasing potential of Tm:Y_2O_3 transparent ceramics at cryogenic temperatures. This gain material can be considered as an alternative gain medium for high average and peak power laser development around 2 μm in nano-second regime.

© 2021 Optical Society of America under the terms of the OSA Open Access Publishing Agreement

1. Introduction

Pulsed lasers generating high energy/power in the 1.8–2.0 μm region based on the $^3F_4 \rightarrow {}^3H_6$ transition of Tm^{3+} (hereafter: Tm) possess broad applications in several fields such as laser induced damage threshold (LIDT) measurement, polymer material processing, remote sensing, medical surgery, pump source for mid-infrared lasers, etc. [1–5]. The advantages of such lasers are mainly due to two reasons: 1) the $^3H_6 \rightarrow {}^3H_4$ transition and 2) the cross-relaxation process. The former can be easily excited by the commercial AlGaAs laser diodes emitting around 800 nm, and the latter increases the laser efficiency by gathering two excited Tm ions for each absorbed pump photon on the $^3F_4$ laser level [6]. However, at room temperature, due to the quasi-three-level nature of Tm ion, the material suffers from reabsorption losses due to the finite population in the $^3H_6$ laser level. This in turn results in higher laser threshold and limits the power scaling capability. In addition, due to the higher energy levels, Tm ions suffer from other unwanted processes like excited state absorption (ESA), energy-transfer up-conversion (ETU), etc., which limit the overall efficiency.

In order to mitigate the above mentioned issues, cooling the active medium down to cryogenic temperatures is a commonly used technique [7–9]. At cryogenic temperature, the lower $^3H_6$ laser level is thermally depopulated, resulting in a four-level-system and consequently reducing the lasing threshold. Besides, with the decrease of temperature, the transition cross-sections of the laser active materials are usually enhanced [10,11]. For example, the increase of stimulated emission cross-section results in a reduced saturation fluence, which is helpful to achieve efficient Q-switched oscillator/amplifier extraction. In addition, the thermo-optical/mechanical properties

#422603 https://doi.org/10.1364/OME.422603
Journal © 2021 Received 11 Feb 2021; revised 31 Mar 2021; accepted 31 Mar 2021; published 21 Apr 2021

Optical Materials EXPRESS

are also improved at cryogenic temperatures [8,9,12]. For example, the thermal conductivity increases whereas the thermal expansion coefficient decreases notably, alleviating the thermal issues such as thermal lensing, thermal induced mechanical stress, etc. Overall, all the above said effects at cryogenic temperatures lead to better laser performance.

To date, many laser studies based on Tm-doped materials have been reported [13–15]. Among the promising hosts, sesquioxides (for example, Lu_2O_3, Y_2O_3, Sc_2O_3 or mixed sesquioxides) either as single crystals or polycrystalline transparent ceramics are of great importance for the high average and peak power (HAPP) laser development. This is mainly due to their high thermal conductivity (13 W/mK for un-doped Y_2O_3 [9]), low phonon energy (~ 600 cm^{-1} [16]) and broad emission band when doped with rare-earth ions [17,18]. Even at 80K, the gain bandwidth of Tm:Y_2O_3 [11] centered at 1932 nm was around 9 nm which is still broad enough to generate transform limited pulses in the nano-second and sub pico-second regime. Nevertheless, obtaining high quality single crystals with such hosts are limited due to the high melting point (> 2400 °C) as well phase transition point below the melting point [19]. Since last decade, more attention on sesquioxides transparent ceramics has been seen owing to the lower fabrication temperature (~ 1800°C), as well the feasibility of producing high quality ceramics with large volume and high dopant concentrations [19,20]. Many studies have been reported for room temperature operation [21–25] and cryogenic investigation of such materials are still under study.

Bearing all the above facts in mind, we intend to develop a high average/peak power (HAPP) laser using cryogenically cooled Tm-doped Y_2O_3 transparent ceramics, for which crucial parameters, such as the exact pump wavelength, operation temperature, lasing threshold, etc., have been reported in our previous work [11]. Here, as a proof of principle, we focus on the pulsed lasing potential and power scaling of the Tm:Y_2O_3 transparent ceramics at liquid nitrogen temperature. The technique employed in this work was based on the master oscillator power amplification (MOPA) concept [26,27].

2. Experimental

2.1. Cryogenic master oscillator setup

The master oscillator was built as illustrated in Fig. 1. The pump source was a volume Bragg grating (VBG) stabilized diode laser (BWT Beijing, Ltd.), which emits at 793.2 nm with a spectral bandwidth of ~ 0.5 nm. In the continuous wave (CW) regime, a maximum output power of 25 W was delivered through a coupled fiber of 105 μm core diameter and numerical aperture N.A. = 0.22. Pulsed pumping was realized by triggering the diode driver using an external digital delay generator (DG645, Stanford Research Systems). The pump radiation was focused onto the active medium in a ratio of 1:2 by two anti-reflectively (AR) coated achromatic lenses (L1 and L2 with focal lengths f of 100 and 200 mm, respectively), resulting in a pump mode size of 210 μm.

In a vacuum chamber, the active medium (an AR-coated 3 at.% Tm:Y_2O_3 transparent ceramic, 3 mm thick and 10 mm in diameter, Konoshima Chemical Co., Ltd) was mounted in a copper holder at normal incidence along the pump direction. Indium foil was placed between the sample and holder for better thermal contact. During the experiments, the sample temperature was cooled down to near liquid nitrogen temperature (80 K) by a closed-cycle helium cryostat (CH-204, JANIS) and the vacuum was maintained below 10^{-6} mbar to avoid any condensation on sample.

The cavity was built by two high-reflectively (HR) coated mirrors (M1 & M3), a dichroic mirror M2, a plano-convex lens L3, a thin film polarizer (TFP), a λ/4-plate and a RTP (Rubidium Titanyl Phosphate) Pockels cell (PC) (Raicol Crystals). The plano-concave mirror M1 had a radius of curvature ROC = - 300 mm, while M3 was a plane mirror. The rear side of M2 was AR coated at the pump wavelength range and the front side was 45° HR coated for both p- and s-polarizations at the laser wavelength. The lens L3, which works as a mode-matching lens in the cavity, had a focal length of 150 mm and was AR coated at the laser wavelength. The TFP highly reflected the s-polarized (vertical-polarized) light and transmitted the p-polarized

Optical Materials EXPRESS

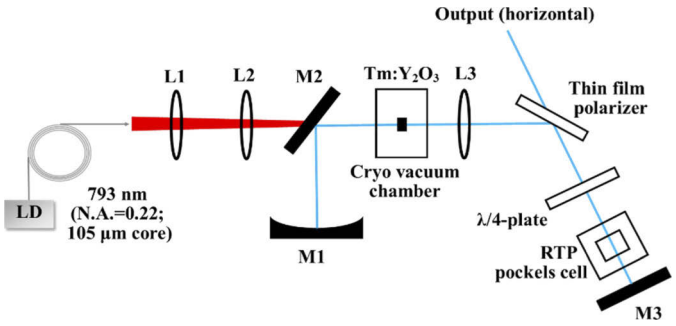

Fig. 1. Experimental setup of the master oscillator: LD - VBG-stabilized pump diode, L1, L2 - achromatic lenses, M1 - HR concave mirror, M2 - dichroic mirror, L3 - AR plano-convex lens, λ/4-plate - quarter wave plate, RTP Pockels cell - electro-optic switch, and M3 – HR plane mirror.

(horizontal-polarized) light fully at a functional angle of 56°.Together with the λ/4-plate, they worked as an adjustable output coupler. The RTP PC was AR-coated for the laser wavelength and worked as an electro-optical switch. It was driven by a home-made high voltage power supply, whose triggering was controlled by the digital delay generator mentioned above.

To generate the pulses, the fast axis of the λ/4-plate was oriented at 45° to the s- and p-polarizations. Thus, the s-polarized light reflected from the TFP was rotated by 90° to the p-direction after a double-pass through the λ/4-plate. In this scenario, when no voltage was applied to the Pockels cell, the M3 back reflected radiation transmitted through the TFP fully. At this time, the cavity had high loss and the inversion population was accumulated in the gain medium. When a λ/4-voltage was applied to the PC, the light reflected from M3 maintained s-polarized after passing through the λ/4-plate and PC. In this phase, the TFP functioned as a total reflective fold mirror resulting in lowering the loss of the cavity, so that the intra-cavity energy was built between the two end-mirrors. After an accumulation time, the λ/4-voltage was removed from the PC and, therefore, all the intra-cavity energy was dumped out through the TFP. In the whole process, the intra-cavity oscillation mode was s-polarized and the output beam was p-polarized.

2.2. Cryogenic double-pass amplifier setup

Amplification process was done using the double-pass geometry, as shown in Fig. 2. The pump diode possesses same parameters as the one used in the oscillator. Pump radiation was imaged onto the active medium in a ratio of 1:6 by the AR coated achromatic lenses L4 and L5 (focal lengths f of 50 and 300 mm, respectively), resulting in a pump beam size of 630 µm. Pulsed pumping was realized by the same digital delay generator and the triggering of the pump was synchronized with the incoming seed pulses. As a gain medium, an AR coated 5 at.% Tm:Y_2O_3 transparent ceramic (3 mm thick and 10 mm in diameter, Konoshima Chemical Co., Ltd) was used to have better absorption of pump wavelength at 80 K. It was mounted at normal incidence to the pump radiation in a home-made vacuum chamber (pressure > 10^{-6} mbar) and the cold finger was cooled by liquid nitrogen (LN_2).

To avoid back-reflection damage to the master oscillator, a Faraday isolator (FI) was placed before the amplifier stage. The double-pass amplification of the seed pulses was realized with the help of a TFP, a λ/4-plate and a curved HR mirror (CM, ROC = −500 mm). The incoming seed light had horizontal polarization and was fully transmitted through the TFP. After being bent by the DM, this horizontally polarized seed radiation passed through the sample and the λ/4-plate for the first time. After the back reflection from the CM, its polarization was changed to

Optical Materials EXPRESS

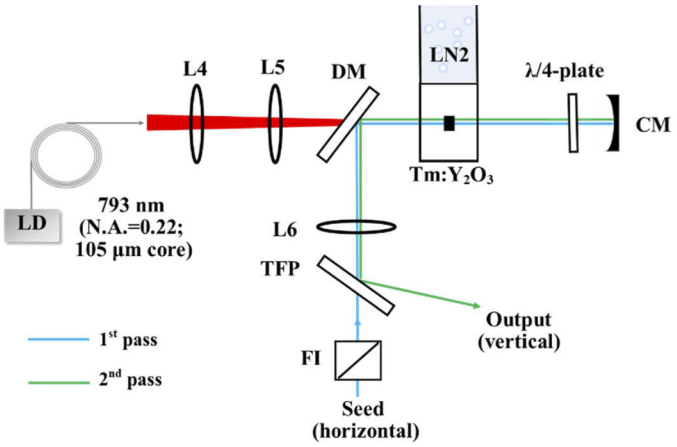

Fig. 2. Experimental setup of a double-pass amplifier: LD - laser diode, L4, L5 - achromatic lenses, DM - dichroic mirror, LN2 - liquid nitrogen, CM - curved mirror, L6 - thin lens, TFP - thin film polarizer, FI - Faraday isolator.

vertical, because of a double-pass through the λ/4-plate. This vertically polarized light passed through the sample for the second time and got totally reflected on the front side of the TFP at an angle of 56°. The thin lens L6 ($f = 250$ mm) and CM adjusted the beam size on the sample. The incoming seed beam size was estimated to be ~ 270 μm by the knife-edge method. Pulse energy, pulse duration and beam profile of the amplified light were monitored by an energy meter (PE25-C, Ophir), an ultrafast photodetector (UPD-3N-IR2-P, Alphalas) and a beam profiling camera (Pyrocam IIIHR, Ophir), respectively.

3. Results and discussion

3.1. Cryogenic master oscillator with tunable repetition rate

Firstly, the distance of optical elements in the oscillator cavity was optimized in CW regime. From the measured distance and using ABCD formalism, the laser mode size was estimated to be around 230 μm. The input-output power characteristics of the optimized cavity with and without the PC were studied and are shown in Fig. 3(a). The maximum CW output power was achieved, when the λ/4-plate fast axis was rotated 12° from the s-polarization (in clockwise). Comparing these two curves in Fig. 3(a), one can see that introducing the PC resulted in almost no extra loss to the cavity. The absorption of the 3 at.% Tm:Y_2O_3 ceramic sample was estimated to be 63.2% at 80 K under non-lasing condition. The laser wavelength was centered at 1932 nm (Fig. 3(b)).

Secondly, with the optimized setup, the pulsed lasing was realized at a repetition rate of 1 to 100 Hz. The pump duration was set as 7 ms to have sufficient population inversion at low pump power. The corresponding pump duty cycles were 0.7, 7, 35 and 70%, for 1, 10, 50 and 100 Hz, respectively. A λ/4-voltage of 1.4 kV was applied to the PC and its accumulation time was set to 50 ns. As shown in Fig. 4(a), the output pulse energy increased linearly with the incident pump energy and no clear variation due to the repetition rate can be observed. This indicates that the active medium was cooled efficiently. The maximum single pulse energy of 1.35 mJ was obtained at 10 Hz. In addition, the average output power with respect to the incident power was estimated and is shown in Fig. 4(b). The output power is free from any thermal rollover. The maximum average output power achieved was 132 mW at 100 Hz. Besides, the measured pulse durations at various repetition rates showed consistency and were measured to be around 30 ns. A typical oscilloscope trace of the 1.35-mJ pulse and its far field beam profile are presented as insets in Figs. 4(a) and 4(b) respectively. The maximum peak power was estimated to be 45 kW at 10 Hz.

Optical Materials EXPRESS

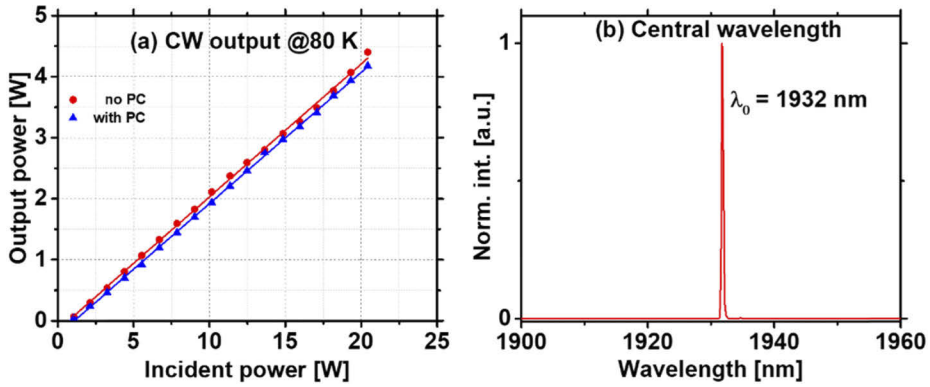

Fig. 3. (a) CW laser output at a λ/4-plate angle of 12°. (b) Laser spectrum of the CW laser.

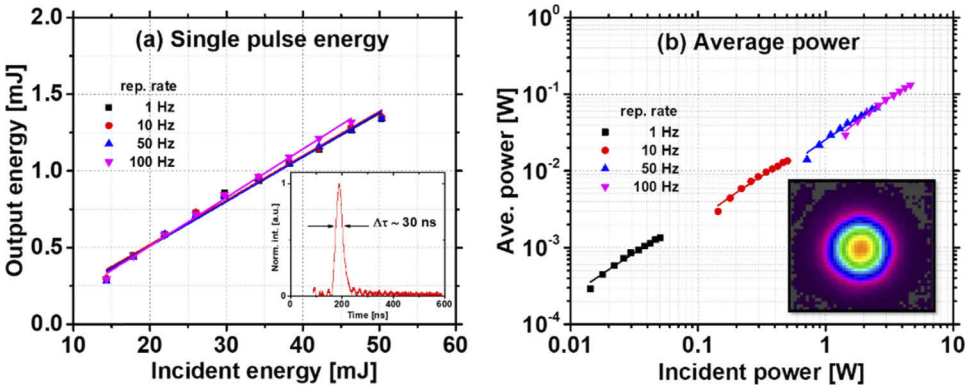

Fig. 4. (a) Output/incident energy characteristics of seed pulses at various rep. rates and (b) the corresponding average power vs. incident pump power. Inset (a) oscilloscope trace of the 1.35-mJ pulse and (b) the corresponding spatial beam profile.

3.2. Cryogenic double-pass amplifier

To amplify the pulse energy, a double-pass geometry as illustrated in the experimental section was executed. The amplification process was characterized by changing three parameters: the amplifier pump duration, the launched seed energy and the repetition rate. In each characterization, we varied one parameter and fixed the other two.

In the first step, the seed pulses of 1 mJ and 10 Hz were injected to the double-pass amplifier stage. The pump duration of the amplifier varied from 3.5 to 14 ms and was synchronized with incoming seed pulses. The absorption of the 5 at.% Tm:Y_2O_3 ceramic sample was estimated to be 79% at 77 K. As shown in Fig. 5(a), after the 1st pass, the single pulse energy was amplified up to ~ 2 mJ. The increase of the pump duration resulted in a small variation of the amplified energy. In contrast, the maximum pulse energy decreased with the increase of pump duration after the 2nd pass, as shown in Fig. 5(b). This decrease of extraction energy may be caused by the insufficient cooling of the gain medium in the amplifier stage.

In the second step, the amplification was characterized with the launched seed energy varying from 0.6 mJ to 1 mJ in a step size of 0.2 mJ. The pump duration and repetition rate were fixed to 3.5 ms and 10 Hz, respectively. As shown in Figs. 5(c) and 5(d), the amplified output pulse energy of both single- and double-pass increased linearly with respect to the incident pump energy for various seed energy. No saturation was observed until the maximum pump energy

Optical Materials EXPRESS

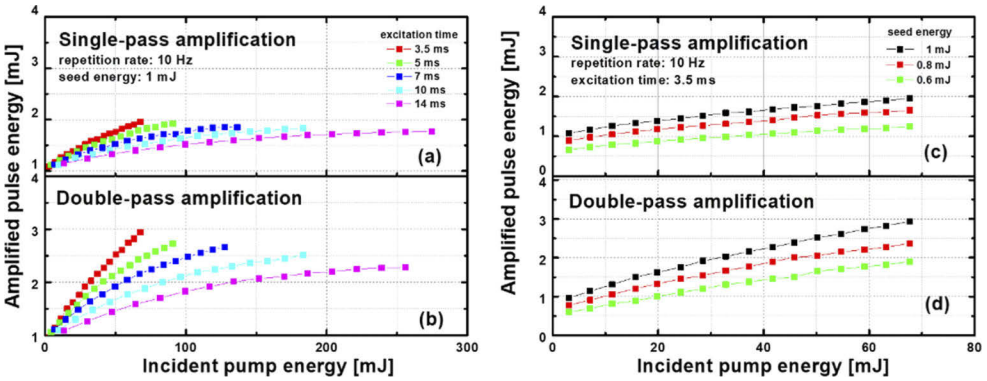

Fig. 5. Amplified output energy characteristics for (a) single-pass and (b) double-pass with different pump durations, and amplified output energy characteristics for (c) single-pass and (d) double-pass with various launched seed energies.

of the laser diode (67.7 mJ). Besides, the increase of seed energy resulted in a clear increase of the amplified output pulse energy. In the single-pass amplification, the maximum amplified pulse energy increased from 1.25 to 1.96 mJ, when the seed energy increased from 0.6 to 1 mJ, whereas, in the double-pass amplification, the maximum amplified pulse energy increased from 1.9 to 2.94 mJ.

In the third step, the amplification was characterized by changing the repetition rate of the seed and pump. The amplifier pump duration was fixed to 3.5 ms and the launched seed energy was set as 1 mJ. The obtained amplified pulse energy values for single- and double-pass are presented in Figs. 6(a) and 6(b), respectively. As shown in Fig. 6(a), the single pulse energy was amplified to the same level at a repetition rate until 50 Hz. Only at 100 Hz, we observed a small reduction for higher incident pump energy, which was also observed in the double-pass amplification (Fig. 6(b)). This decrease at 100 Hz was mainly caused by the increased pump duty cycle, which resulted in more heat generation in the sample. Cryostats with higher cooling capacity will greatly help in overcoming such a thermal issue at high repetition rates.

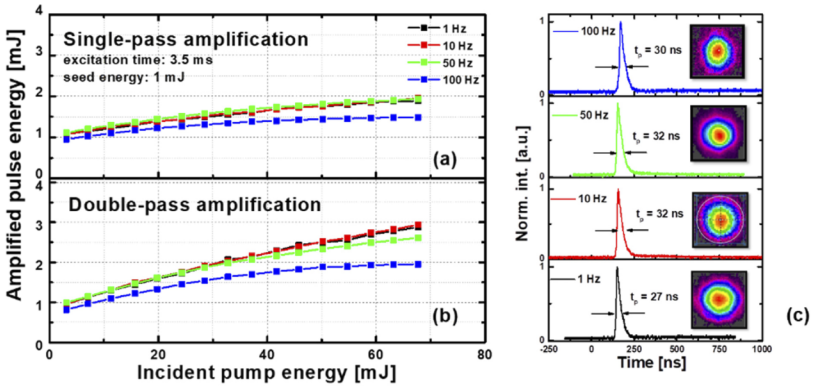

Fig. 6. Amplified output energy characteristics of (a) single-pass and (b) double-pass for various repetition rates. (c) Oscilloscope trace of double-pass amplified pulses obtained at various repetition rates, insets: the corresponding far field beam profiles.

The pulse duration and corresponding beam profile measured at maximum pulse energy are shown in Fig. 6(c). The pulse duration was around 30 ns for all repetition rates. Accordingly, the

Optical Materials EXPRESS

maximum peak power after the double-pass amplification was estimated to be 107, 92, 82 and 65 kW for 1, 10, 50 and 100 Hz, respectively. As the insets in Fig. 6(c) show, the obtained far field beam profiles are high quality Gaussian single mode for each repetition rate. The amplified pulse wavelength was 1932 nm, which matches well with the input seed wavelength as mentioned earlier.

4. Summary

As a proof of principle, we demonstrated a 2 µm MOPA laser system based on cryogenically cooled Tm:Y_2O_3 transparent ceramics for the first time. The master oscillator can be tunable from 1 to 100 Hz. A maximum pulse energy of 1.35 mJ with a pulse duration of 30 ns amounting to a peak power of 45 kW were obtained at 10 Hz. As a power amplifier, using double-pass geometry and seed pulses of 1 mJ, a maximum single pulse energy of 2.94 mJ was achieved at 10 Hz under the incident pump energy of 67.7 mJ. A maximum peak power of 107 kW was obtained at 1 Hz with a pulse duration of 27 ns. The achieved results showed the pulsed lasing potential of Tm:Y_2O_3 transparent ceramics at cryogenic temperatures. Thus, such material can be considered as an alternative gain medium for two-micron HAPP laser development in nano-second regime. Further work will be focused on four-pass geometry to increase the amplified output energy.

Funding. Ministerstvo Školství, Mládeže a Tělovýchovy (Programs NPU I Project No. LO1602); Horizon 2020 Framework Programme (739573); European Regional Development Fund (CZ.02.1.01/0.0/0.0/15_006/0000674).

Acknowledgments. We dedicate this work in memory of our late colleague Dr. Antonio Lucianetti, Head of Advanced Laser Development department, HiLASE Center. He left this world calmly on Nov 19, 2020, in Bergamo, Italy, at the age of 55 after a short and insidious illness.

Disclosures. The authors declare no conflicts of interest.

References

1. K. Scholle, P. Fuhrberg, P. Koopmann, and S. Lamrini, "2 µm laser sources and their possible applications," in B. Pal (Ed.), *Frontiers in Guided Wave Optics and Optoelectronics* (INTECH Open Access Publisher, 2010), Ch. 21.
2. C. Zhu, V. Dyomin, N. Yudin, O. Antipov, G. Verozubova, I. Eranov, M. Zinoviev, S. Podzyvalov, Y. Zhuravlyova, Y. Slyunko, and C. Yang, "Laser-induced damage threshold of nonlinear GaSe and GaSe:In crystals upon exposure to pulsed radiation at a wavelength of 2.1 µm," Appl. Sci. **11**(3), 1208 (2021).
3. U. N. Singh and Jirong Yu, "2-micron laser development for space-based remote sensing applications," in *International Conference on Recent Advances in Space Technologies, RAST*, Proceedings of Istanbul (2003), pp. 485–487.
4. V. A. Akimov, V. Kozlovsky, Y. V. Korostelin, A. I. Landman, Y. Podmar'kov, Y. K. Skasyrskii, and M. Frolov, "Efficient pulsed Cr^{2+}:CdSe laser continuously tunable in the spectral range from 2.26 to 3.61," Quantum Electron. **38**(3), 205–208 (2008).
5. K. Yang, Y. Yang, J. He, and S. Zhao, *Q-Switched 2 Micron Solid-State Lasers and Their Applications* [online first] (IntechOpen, 2019).
6. M. Schellhorn, "High-power diode-pumped Tm:YLF laser," Appl. Phys. B **91**(1), 71–74 (2008).
7. T. Y. Fan, D. J. Ripin, R. L. Aggarwal, and J. R. Ochoa, C. Bien, M. Tilleman, and J. Spitzberg, "Cryogenic Yb^{3+}-doped solid-state lasers," IEEE J. Sel. Top. Quant. **13**(3), 448–459 (2007).
8. D. C. Brown, S. Tornegard, J. Kolis, C. McMillen, C. Moore, L. Sanjeewa, and C. Hancock, "The application of cryogenic laser physics to the development of high average power ultra-short pulse lasers," Appl. Sci. **6**(1), 23 (2016).
9. D. Brown, S. Tornegård, and J. Kolis, "Cryogenic nanosecond and picosecond high average and peak power (HAPP) pump lasers for ultrafast applications," High Power Laser Sci. Eng. **4**, e15 (2016).
10. J. Reiter, J. Körner, J. Pejchal, A. Yoshikawa, J. Hein, and M. C. Kaluza, "Temperature dependent absorption and emission spectra of Tm:CaF_2," Opt. Mater. Express **10**(9), 2142–2158 (2020).
11. F. Yue, V. Jambunathan, S. Paul David, X. Mateos, M. Aguiló, F. Díaz, J. Šulc, A. Lucianetti, and T. Mocek, "Spectroscopy and diode-pumped continuous-wave laser operation of Tm:Y_2O_3 transparent ceramic at cryogenic temperatures," Appl. Phys. B **126**(3), 44 (2020).
12. V. Cardinali, E. Marmois, B. Le Garrec, and G. Bourdet, "Determination of the thermo-optic coefficient dn/dT of ytterbium doped ceramics (Sc_2O_3, Y_2O_3, Lu_2O_3, YAG), crystals (YAG, CaF_2) and neodymium doped phosphate glass at cryogenic temperature," Opt. Mater. **34**(6), 990–994 (2012).
13. Y. Zhang, B. Yao, T. Dai, H. Shi, L. Han, Y. Shen, and Y. Ju, "Electro-optically cavity-dumped 3 ns Tm:LuAG laser," Appl. Opt. **55**(11), 2848–2851 (2016).
14. L. Jin, P. Liu, H. Huang, X. Liu, and D. Shen, "Short pulse diode-pumped Tm:YAG slab laser electro-optically Q-switched by $RbTiOPO_4$ crystal," Opt. Mater. **60**, 350–354 (2016).

Optical Materials EXPRESS

15. S. Ma, D. Lu, H. Yu, H. Zhang, X. Han, Q. Lu, C. Ma, and J. Wang, "Langasite electro-optic Q-switched 2μm laser with high repetition rates and reduced driven voltages," Opt. Commun. **447**, 13–17 (2019).
16. C. Kraenkel, "Rare-earth-doped sesquioxides for diode-pumped high-power lasers in the 1-, 2-, and 3-μm spectral range," IEEE J. Sel. Top. Quantum Electron. **21**, 250–262 (2015).
17. M. Tokurakawa, A. Shirakawa, K. Ueda, H. Yagi, T. Yanagitani, A. A. Kaminskii, K. Beil, C. Kränkel, and G. Huber, "Continuous wave and mode-locked Yb^{3+}:Y_2O_3 ceramic thin disk laser," Opt. Express **20**(10), 10847–10853 (2012).
18. P. Loiko, P. Koopmann, X. Mateos, J. M. Serres, V. Jambunathan, A. Lucianetti, T. Mocek, M. Aguilo, F. Diaz, U. Griebner, V. Petrov, and C. Kraenkel, "Highly efficient, compact Tm^{3+}:RE_2O_3 (RE = Y, Lu, Sc) sesquioxide lasers based on thermal guiding," IEEE J. Sel. Top. Quantum Electron. **24**(5), 1–13 (2018).
19. A. Pirri, G. Toci, B. Patrizi, and M. Vannini, "An overview on Yb-doped transparent polycrystalline sesequioxide laser ceramics," IEEE J. Sel. Top. Quant. **24**, 160218 (2018).
20. S. F. Wang, J. Zhang, D. W. Luo, F. Gu, D. Y. Tang, Z. L. Dong, G. E. B. Tan, W. X. Que, T. S. Zhang, S. Li, and L. B. Kong, "Transparent ceramics: processing, materials and applications," Prog. Solid State Chem. **41**(1-2), 20–54 (2013).
21. O. L. Antipov, A. A. Novikov, N. G. Zakharov, and A. P. Zinoviev, "Optical properties and efficient laser oscillation at 2066nm of novel Tm:Lu_2O_3 ceramics," Opt. Mater. Express **2**(2), 183–189 (2012).
22. P. A. Ryabochkina, A. N. Chabushkin, Y. L. Kopylov, V. V. Balashov, and K. V. Lopukhin, "Two-micron lasing on diode-pumped Y_2O_3: Tm ceramics," Quantum Electron. **46**(7), 597–600 (2016).
23. H. Huang, H. Wang, and D. Shen, "VBG-locked continuous-wave and passively Q-switched Tm:Y_2O_3 ceramic laser at 2.1 μm," Opt. Mater. Express **7**(9), 3147–3154 (2017).
24. H. Wang, H. Huang, P. Liu, L. Jin, D. Shen, J. Zhang, and D. Tang, "Diode-pumped continuous-wave and Q-switched Tm:Y_2O_3 ceramic laser around 2050nm," Opt. Mater. Express **7**(2), 296–303 (2017).
25. X. Xu, Z. Hu, D. Li, P. Liu, J. Zhang, B. Xu, and J. Xu, "First laser oscillation of diode-pumped Tm^{3+}-doped $LuScO_3$ mixed sesquioxide ceramic," Opt. Express **25**(13), 15322–15329 (2017).
26. A. Agnesi, P. Dallocchio, F. Pirzio, and G. Reali, "Sub-nanosecond single-frequency 10-kHz diode-pumped MOPA laser," Appl. Phys. B **98**(4), 737–741 (2010).
27. R. C. Stoneman, R. Hartman, E. A. Schneider, C. G. Garvin, and S. W. Henderson, "Efficient diffraction-limited SLM eyesafe 1617 nm Er:YAG MOPA with 1.1 ns pulsewidth," in *Advanced Solid-State Photonics, OSA Technical Digest Series (CD)* (Optical Society of America, 2007), paper WE2.